IEEE Access
Multidisciplinary : Rapid Review : Open Access Journal

SPECIAL SECTION ON ADVANCED MODELING AND CONTROL OF COMPLEX MECHATRONIC SYSTEMS WITH NONLINEARITY AND UNCERTAINTY

Received April 21, 2018, accepted May 20, 2018, date of publication May 25, 2018, date of current version June 20, 2018.

Digital Object Identifier 10.1109/ACCESS.2018.2840519

Adaptive Fuzzy Sliding Mode Observer for Cylinder Mass Flow Estimation in SI Engines

CHANGHUI WANG[1], MEI LIANG[1], AND CHUN-NA LI[2]
[1]School of Electromechanical and Automotive Engineering, Yantai University, Yantai 264005, China
[2]Zhijiang College, Zhejiang University of Technology, Hangzhou 310024, China

Corresponding authors: Mei Liang (mmglm@163.com) and Chun-Na Li (na1013na@163.com)

This work was supported in part by the Foundation of State Key Laboratory of Automotive Simulation and Control under Grant 20171105, in part by the National Natural Science Foundation of China under Grants 61703370, 61703179, and 61573165, and in part by the Zhejiang Provincial Natural Science Foundation of China under Grant LQ17F030003.

ABSTRACT In this paper, a novel algorithm for the cylinder mass flow estimation in four-stroke spark ignition (SI) gasoline engines is developed to improve the estimation precision under transient conditions. The error of the cylinder mass flow is compensated by the error variable of the volumetric efficiency caused by the calibration errors and ambient changes. Since the volumetric efficiency error in SI gasoline engines is dependent on the intake manifold pressure, engine speed, and ambient temperature, a fuzzy logic system (FLS) with three inputs is adopted to parameterize the volumetric efficiency error. With the combination of the FLS and the gasoline engine air path system, an adaptive fuzzy sliding mode observer is presented to estimate the states and parameters jointly and suppress the disturbance from the FLS approximation error. With the conditions of persistent excitation and the given inequality, the convergence of the proposed method is proven. The performance of the proposed method is validated in the environment of a R4-cylinder SI gasoline engine from enDYNA during different driving-cycle conditions, demonstrating that the estimation precision of the cylinder air inflow can be obviously improved by the proposed algorithm under transient conditions.

INDEX TERMS SI gasoline engine, cylinder mass flow, volumetric efficiency, fuzzy logic system, adaptive fuzzy sliding mode observer.

I. INTRODUCTION

Spark ignition (SI) gasoline engines are extensively used as a power source for passenger vehicles because of their small size, small vibration and stable operation, but have emissions problems (HC, CO and NOx) limited by stringent emission regulations and restrictive standards [1]–[3]. Three-way catalysts (TWC) equipped on SI gasoline engines are applied to reduce the emissions and satisfy stringent emissions regulations. In order to convert all HC, CO and NOx emissions to the innocuous components water and carbon dioxide, the engine air-to-fuel ratio (AFR) has to be controlled to very narrow AFR band around stoichiometry, in which the maximum TWC emissions conversion efficiency is achieved [4], [5].

AFR control is based on a combined feed-forward and feed-back technique in the engine control units (ECUs) to obtain both good transient and steady-state responses [6], [7]. In the feed-forward system, the cylinder mass flow is estimated based on a combination of sensor measurements and volumetric efficiency map, and then the quantity of fuel injection is decided by ECUs to achieve the target AFR. Therefore, accurate estimation of the cylinder mass flow under all different operating conditions is required to inject proper fuel [8]. For the feed-back control, the universal exhaust gas oxygen (UEGO) sensor installed in the exhaust manifold is adopted to measure the oxygen content in the exhaust stream pre-catalyst, and provide feedback on AFR errors used to adjust the fuel injection quantity, by which the feed-back methods can work well during steady-state conditions. Due to the time-varying transport delay from the exhaust confluence point to the UEGO sensor as well as the sensor delay caused by UEGO sensor response [9], the feed-back strategies are limited under transient conditions. Therefore, under transient conditions, the accurate estimation of the cylinder mass flow in feed-forward is very important to avoid large AFR errors and reduce the engine emissions.

Ideally, the cylinder mass flow is equal to the product of the atmospheric air density and the cylinder displacement volume. However, the amount of air enters the cylinders is less than the ideal amount, due to the short cycle time and the flow restrictions from the air filter, intake manifold, and intake valves. Therefore, the rate between the actual cylinder air mass flowing and the theoretical cylinder air mass is defined as volumetric efficiency [4], [10]. An accurate cylinder mass flow estimation model can be obtained through the accurate volumetric efficiency. In fact, there is a nonlinear function relationship between the volumetric efficiency and the engine-related parameters [11]. To describe the volumetric efficiency in the engine ECUs, the map (or lookup table [12]) with the advantage of the low computational load is used to store the values of the volumetric efficiency at each engine operating point. Using the engine dynamometer, the map is calibrated under steady-state conditions and room temperature ambient conditions [11], [13], [14].

Due to the ambient changes and the increased engine complexity (such as variable valve timing), the volumetric efficiency map is subjected to modeling errors, leading to adverse impacts on the emission performance of gasoline engines [8]. Naturally, an accurate compensation map for the volumetric efficiency error can benefit the cylinder mass flow estimation. However, a large number of static bench-test data under steady-state conditions is required to calibrate the error map, which is expensive because of the test bench occupation and operator working time [15], [16]. To avoid error map calibration and reduce the vehicle development cycle time, an unknown input observer based on the intake manifold dynamics is designed to estimate the additive error of the volumetric efficiency in both steady-state and transient conditions [17], [18]. However, owing to the volumetric efficiency error considered as a constant in the unknown input observer, the bound of the estimate error is proportional to the rate of the volumetric efficiency error, in which the estimation precision of the volumetric efficiency error can be reduced under rapid transient conditions. The sliding-mode technology has been researched and used extensively [19]–[21]. In [22], an adaptive sliding-mode observer is proposed to estimate the cylinder mass flow using the sliding-mode methodology, in which the large modeling error of the volumetric efficiency can destroy the performance in terms of the accuracy and the response time. In fact, due to the input-output relationship of the volumetric efficiency map, the volumetric efficiency error is a nonlinear function of engine-related parameters. Therefore, under transient conditions, the estimation of the volumetric efficiency error considered as a constant brings adverse impacts on the estimation performance of the cylinder mass flow.

Fuzzy logic systems (FLSs) have been proved to be an effective and flexible tool for approximation of the nonlinear model, which have been widely used for nonlinear identification and control and achieved good control performance (see, for example, [23]–[25]). According to the Stone-Weierstrass theorem, a universal fuzzy approximator can approximate any real continuous function on a compact set to an arbitrary degree of accuracy.

To improve the estimation precision of the cylinder mass flow under engine transient conditions, a FLS (with the intake manifold pressure, engine speed and ambient temperature as three inputs) is adopted to parameterize the nonlinear function relationship of volumetric efficiency error, thus the function estimation of the volumetric efficiency error becomes the problem of parameter estimation. With the combination of the FLS and the engine air path system, an adaptive fuzzy sliding mode is designed, which achieves the joint estimation of the system state and the unknown parameters form FLS, as well as the disturbance suppression for the approximation error from the parameterization. Under the given conditions, the convergence of the proposed algorithm is proven. The simulation study of the proposed algorithm compared with the unknown input observer in [17] and adaptive sliding-mode observer in [22] is presented in the environment of 2.0L R4-cylinder SI gasoline engine with 4-stroke from enDYNA under FTP75 cycle and ECE cycle respectively. The results demonstrate that the estimation precision of the cylinder mass flow under transient condition is obviously improved by the proposed method under transient conditions.

This paper is organized as follows. In Section 2, the volumetric efficiency error is parameterized by FLS, and the joint estimation problem for the engine air path system is given. In Section 3, the adaptive fuzzy sliding mode observer is proposed, as well as the analysis of the convergence of the parameter estimation. Simulation results from enDYNA are presented in Section 4, and the conclusions are summarized in Section 5.

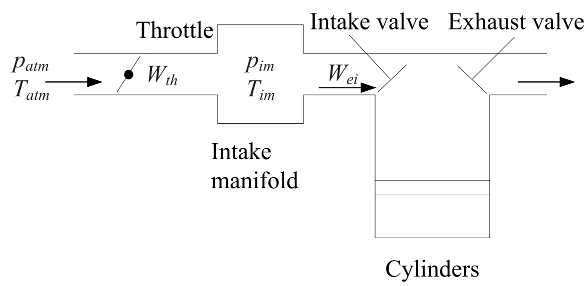

FIGURE 1. Schematic of the naturally aspirated SI gasoline engine.

II. PROBLEM FORMULATION AND PRELIMINARIES

A. PROBLEM FORMULATION

Fig. 1 shows the model structure of a naturally aspirated spark ignition (SI) gasoline engine, and the model can be expressed as [5], [11]:

$$\dot{p}_{im} = \frac{R_a T_{im}}{\mathrm{V}_{im}} (W_{th} - W_{ei}) \tag{1}$$

where

$$W_{ei} = \frac{\eta_v p_{im} n_e V_d}{120 R_a T_{im}}, \quad W_{th} = \frac{C_d(n_e, u_{th}) p_{amb} A(u_{th}) \Psi(\Pi)}{\sqrt{R_a T_{amb}}},$$
$$\Pi = \frac{p_{im}}{p_{atm}}$$

$$C_d\left(n_e, u_{th}\right) = c_0 b_0\left(1+\frac{b_1}{b_0} n_e\right)+c_1 b_0\left(1+\frac{b_1}{b_0} n_e\right) u_{th} + c_2 b_0\left(1+\frac{b_1}{b_0} n_e\right) u_{th}^2$$

$$A\left(u_{th}\right)=\frac{\pi D^2}{4} \cdot\left(1-\cos \left(u_{th}+u_{th0}\right)\right)$$

$$\Psi(\Pi)=\begin{cases}\sqrt{\Pi^{\frac{2}{\gamma}}-\Pi^{\frac{\gamma+1}{\gamma}}}, & \Pi>\left(\frac{2}{\gamma+1}\right)^{\frac{\gamma}{\gamma-1}} \\ \sqrt{\left(\frac{2}{\gamma+1}\right)^{\frac{2}{\gamma-1}}-\left(\frac{2}{\gamma+1}\right)^{\frac{\gamma+1}{\gamma-1}}}, & \Pi \leq\left(\frac{2}{\gamma+1}\right)^{\frac{\gamma}{\gamma-1}}\end{cases} \tag{2}$$

where W_{th} is the throttle mass air flow, W_{ei} is the cylinder mass flow, η_v is the volumetric efficiency, n_e is the engine speed, u_{th} is the throttle angle, γ is the air specific heat capacity ratio, D is the diameter of the throttle body throat, p_{amb}, T_{amb} are the ambient pressure and temperature, p_{im}, T_{im} are the intake manifold pressure and temperature, R_a is the gas constant, C_d is the flow coefficient of the throttle body throat, u_{th0} is the offset angle of the throttle and c_0, c_1, c_2, b_0, b_1 are the model parameters.

Due to the ambient changes and the increased engine complexity, the volumetric efficiency η_v is subjected to modeling errors. Considering the model error of volumetric efficiency η_v, η_v is recorded as:

$$\eta_v=\eta_{vk}+\Delta \eta_v \tag{3}$$

where η_{vk} is the modeled term of the volumetric efficiency, and $\Delta\eta_v$ is the error of the volumetric efficiency.

The volumetric efficiency η_v of the naturally aspirated SI gasoline engine is mainly dependent on the intake manifold pressure p_{im}, engine speed n_e and ambient temperature T_{amb} [11], so the volumetric efficiency error $\Delta\eta_v$ is also dependent on the intake manifold pressure p_{im}, engine speed n_e and ambient temperature T_{amb}, i.e., $\Delta\eta_v\left(p_{im}, n_e, T_{amb}\right)$.

The purpose of this paper is the estimation of the unknown error function $\Delta\eta_v\left(p_{im}, n_e, T_{amb}\right)$ to compensate the volumetric efficiency model η_{vk} and improve the precision of the cylinder mass flow W_{ei}. To improve the estimation precision of the error function $\Delta\eta_v\left(p_{im}, n_e, T_{amb}\right)$ under engine transient conditions, the nonlinear function relationship $\Delta\eta_v\left(p_{im}, n_e, T_{amb}\right)$ is parameterized by the FLS with unknown parameters in the following.

B. FUZZY LOGIC SYSTEM APPROXIMATION AND SYSTEM TRANSFORMATION

The FLSs can be used as practical function approximators from a mathematical point of view. Thus, a FLS can be used to approximate a continuous function $f(x)$ defined on some compact set [26].

There are consists of four parts in a FLS: the knowledge base, the fuzzifier, the fuzzy inference engine and the defuzzifier. The knowledge base is composed of a collection of fuzzy IF-THEN rules of the following form:

R^l: if x_1 is F_1^l and x_2 is $F_2^l \cdots$ and x_n is F_n^l, then y is G^l, $l=1,2,\ldots,N$

where $x=[x_1, \ldots, x_n]^{\mathrm{T}}$ is FLS input, and y is FLS output. N is the number of inference rules. $\mu_{F_i^l}(x_i)$ and $\mu_{G^l}(y)$ are the membership functions of fuzzy sets F_i^l and G^l, respectively. Through singleton fuzzifier, center average defuzzification and product inference, the FLS can be expressed as

$$y(x)=\frac{\sum_{l=1}^N \bar{y}_l\left(\prod_{i=1}^n \mu_{F_i^l}\left(x_i\right)\right)}{\sum_{l=1}^N\left(\prod_{i=1}^n \mu_{F_i^l}\left(x_i\right)\right)} \tag{4}$$

where $\bar{y}_l=\max\limits_{y \in R} \mu_{G^l}(y)$. Define the fuzzy basis functions as

$$\varphi_l(x)=\frac{\prod_{i=1}^n \mu_{F_i^l}\left(x_i\right)}{\sum_{l=1}^N\left(\prod_{i=1}^n \mu_{F_i^l}\left(x_i\right)\right)}, \quad l=1,2,\ldots,N \tag{5}$$

Denoting $\theta^{\mathrm{T}}=[\bar{y}_1, \bar{y}_2, \ldots, \bar{y}_N]=[\theta_1, \theta_2, \ldots, \theta_N]$ and $\varphi(x)=[\varphi_1(x), \varphi_2(x), \ldots, \varphi_N(x)]^{\mathrm{T}}$. Then, FLS (4) can be rewritten as

$$y(x)=\theta^{\mathrm{T}} \varphi(x) \tag{6}$$

Lemma 1 [27]: For any continuous function $f(x)$ defined over a compact set Ω and any given positive constant ε, there exists a FLS (6) and an ideal parameter vector θ^* such that

$$\sup_{x \in \Omega}\left|f(x)-\theta^{*\mathrm{T}} \varphi(x)\right| \leq \varepsilon \tag{7}$$

According to Lemma 1, FLSs are universal approximators to approximate any smooth functions on a compact space. Therefore, the nonlinear terms $\Delta\eta_v$ in (3) can be approximated by the following FLSs:

$$\Delta \eta_v\left(\upsilon \mid \theta_{\Delta \eta}\right)=\theta_{\Delta \eta}^{\mathrm{T}} \varphi_{\Delta \eta}(\upsilon) \tag{8}$$

where $\upsilon=\left(p_{im}, n_e, T_{amb}\right)$. The optimal parameter vectors $\theta_{\Delta\eta}^*$ is defined as

$$\theta_{\Delta \eta}^*=\arg \min_{\theta_{\Delta \eta} \in \Omega}\left[\sup_{\hat{\upsilon} \in V}\left|\Delta \hat{\eta}_v\left(\hat{\upsilon} \mid \theta_{\Delta \eta}\right)-\Delta \eta_v(\hat{\upsilon})\right|\right] \tag{9}$$

where Ω and V are bounded compact sets for $\theta_{\Delta\eta}$ and $\hat{\upsilon}$, respectively.

The corresponding fuzzy minimum approximation error $\varepsilon_{\Delta\eta}$ is defined by

$$\varepsilon_{\Delta \eta}=\Delta \eta_v(\hat{\upsilon})-\Delta \hat{\eta}_v\left(\hat{\upsilon} \mid \theta_{\Delta \eta}^*\right) \tag{10}$$

By substituting (8)-(10) into (1), the system given in (1) can be presented in the following form:

$$\begin{cases}\dot{x}=f\left(\upsilon, u_{th}\right)+\theta_{\Delta \eta}^{\mathrm{T}} \varphi(\upsilon)+R_{\Delta \eta} \\ y=C x\end{cases} \tag{11}$$

where

$$x = p_{im}, \quad C = 1, \ \varphi(\upsilon) = -\frac{V_d p_{im} n_e}{120 \mathrm{V}_{im}} \varphi_{\Delta\eta}(\upsilon)$$
$$f(\upsilon, u_{th}) = \frac{R_a T_{im}}{\mathrm{V}_{im}} W_{th}(p_{im}, n_e, u_{th}) - \frac{\eta_{vk} p_{im} n_e V_d}{120 \mathrm{V}_{im}}$$
$$R_{\Delta\eta} = -\frac{V_d p_{im} n_e}{120 \mathrm{V}_{im}} \varepsilon_{\Delta\eta}, \quad \upsilon = (p_{im}, n_e, T_{amb})$$

Eq. (11) indicates that the estimation of the volumetric efficiency error $\Delta\eta_v(p_{im}, n_e, T_{amb})$ becomes a joint estimation of state x and unknown parameter $\theta_{\Delta\eta}$ for system (11) with the disturbance $R_{\Delta\eta}$ from the approximation error $\varepsilon_{\Delta\eta}$.

C. ADAPTIVE FUZZY SLIDING MODE OBSERVER DESIGN

Adaptive sliding mode observer is a recursive algorithm to jointly the estimate system state and unknown parameters, which can simultaneously reject the disturbance from the model uncertainty and external signal [28], [29]. The adaptive fuzzy sliding mode observer for the system (11) to jointly estimate the system state and parameters is designed as follows:

$$\begin{cases} \dot{\hat{x}} = f(\upsilon, u_{th}) + \hat{\theta}_{\Delta\eta}^{\mathrm{T}} \varphi_{\Delta\eta}(\upsilon) + L(y - C\hat{x}) + \alpha(t; \hat{x}, y) \\ \dot{\hat{\theta}}_{\Delta\eta} = \Gamma \varphi_{\Delta\eta}(\upsilon) P(y - C\hat{x}) \end{cases} \tag{12}$$

where $\hat{x} \in \mathbb{R}$ is the state estimate, $\hat{\theta}_{\Delta\eta} \in \mathbb{R}^p$ is the parameter estimate, $L \in \mathbb{R}^{3\times 3}$ is the feedback gain matrix, gain $\Gamma \in \mathbb{R}^{p\times p}$ is the positive definite diagonal matrix, and a sliding mode control law of

$$\alpha(t; \hat{x}, y) = \begin{cases} l_\alpha \dfrac{(y - C\hat{x})}{2\left\|(y - C\hat{x})\right\|} & , \left\|(y - C\hat{x})\right\| \geq \varepsilon_\alpha \\ 0 & , \left\|(y - C\hat{x})\right\| < \varepsilon_\alpha \end{cases} \tag{13}$$

where l_α is a positive gain and ε_α is a small positive constant.

As the intake manifold pressure p_{im}, engine speed n_e and ambient temperature T_{amb} are continuous and bounded in nature, and the model error $\varepsilon_{\Delta\eta}$ is bounded, the following assumption 1 can be satisfied to analyze the convergence of the proposed observer.

Assumption 1: There is unknown positive constant d_R such that $\left|R_{\Delta\eta}\right| \leq d_R$.

The asymptotical stability of the presented method (12) is analyzed in the following theorem.

Theorem 1: If $\exists l_\alpha > 2d_s$, and the following conditions 1) and 2) hold, then adaptive fuzzy sliding mode observer (12) is asymptotically stable, i.e., for any initial conditions $x(0), \hat{x}(0), \hat{\theta}_{\Delta\eta}(0)$ and parameter vector $\theta_{\Delta\eta} \in \mathbb{R}^p$, the errors $\hat{x} - x$ and $\hat{\theta}_{\Delta\eta} - \theta_{\Delta\eta}$ tend to zero asymptotically when $t \to \infty$.

1). There exist matrices $L, P = P^{\mathrm{T}} > 0, Q = Q^{\mathrm{T}} > 0$, such that the following linear matrix inequality (LMI) is feasible:

$$-C^{\mathrm{T}} L^{\mathrm{T}} P - PLC < -Q \tag{14}$$

2). Regression vector $\varphi(\upsilon)$ is persistently exciting, i.e., $\exists \delta_1, \delta_2 > 0; \exists T > 0; \forall t \geq 0$:

$$\delta_1 I_p \leq \int_t^{t+T} \varphi(\upsilon(\tau)) \varphi(\upsilon(\tau))^{\mathrm{T}} d\tau \leq \delta_2 I_p \tag{15}$$

Proof: Set the estimation error

$$\tilde{x} = \hat{x} - x, \tilde{\theta}_{\Delta\eta} = \hat{\theta}_{\Delta\eta} - \theta_{\Delta\eta} \tag{16}$$

Notice that $\dot{\theta}_{\Delta\eta} = 0$, the error dynamic system between (16) and (12) is

$$\begin{cases} \dot{\tilde{x}} = (-LC)\tilde{x} + \tilde{\theta}_{\Delta\eta}^{\mathrm{T}} \varphi(\upsilon) + \alpha - R_{\Delta\eta} \\ \dot{\tilde{\theta}}_{\Delta\eta} = -\Gamma \varphi(\upsilon) P\tilde{x} \end{cases} \tag{17}$$

The Lyapunov function candidate is considered as $V = \tilde{x}^{\mathrm{T}} P\tilde{x} + \tilde{\theta}_{\Delta\eta}^{\mathrm{T}} \Gamma^{-1} \tilde{\theta}_{\Delta\eta}$, and the derivative of V along with the error dynamic system (17) is

$$\begin{aligned} \dot{V} &= 2\tilde{x}^{\mathrm{T}} P\dot{\tilde{x}} + 2\tilde{\theta}_{\Delta\eta}^{\mathrm{T}} \Gamma^{-1} \dot{\tilde{\theta}}_{\Delta\eta} \\ &= 2\tilde{x}^{\mathrm{T}} P(-LC)\tilde{x} + 2\tilde{x}^{\mathrm{T}} P\alpha - 2\tilde{x}^{\mathrm{T}} PR_{\Delta\eta} \end{aligned} \tag{18}$$

According to Assumption 1 and Eq. (13), the following inequalities hold:

$$\begin{aligned} -2\tilde{x}^{\mathrm{T}} PR_{\Delta\eta} &\leq 2d_R \left\|\tilde{x}^{\mathrm{T}} P\right\| \\ 2\tilde{x}^{\mathrm{T}} P\alpha &= l_\alpha \frac{\tilde{x}^{\mathrm{T}} P(y - C\hat{x})}{\left\|(y - C\hat{x})\right\|} = -l_\alpha \left\|P\tilde{x}\right\| \end{aligned} \tag{19}$$

According to condition 1), Eqs. (18) and (19), the following inequality holds:

$$\dot{V} = \tilde{x}^{\mathrm{T}} \left((-LC)^{\mathrm{T}} P + P(-LC)\right)\tilde{x} \leq -\tilde{x}^{\mathrm{T}} Q\tilde{x} < 0 \tag{20}$$

That is $\dot{V} < -\omega(t) < 0$, where $\omega(t) = \tilde{x}^{\mathrm{T}} Q\tilde{x}$.

Therefore, the equilibrium $\tilde{x} = 0$ and $\tilde{\theta}_{\Delta\eta} = 0$ are stable. Now integrate $\dot{V} < -\omega(t)$ from zero to t yields

$$V(t) + \int_0^t \omega(\tau) d\tau < V(0) \tag{21}$$

This means that $\int_0^t \omega(\tau) d\tau < V(0)$ since $V > 0$. So we have $\lim\limits_{t\to\infty} \int_0^t \omega(\tau) d\tau \leq V(0)$ and this implies that $\lim\limits_{t\to\infty} \int_0^t \omega(\tau) d\tau$ exists and is finite. By *Barbalat's* Lemma [30], we know that $\lim\limits_{t\to\infty} \omega(t) = 0$ and this leads to $\lim\limits_{t\to\infty} \tilde{x}(t) = 0$.

Under condition 2), the vector $\varphi(\upsilon)$ is persistently exciting, that is $\lim\limits_{t\to\infty} \tilde{\theta}_{\Delta\eta}(t) = 0$ [30].

Remark 1: According to Theorem 1, the model error $R_{\Delta\eta}$ from $\varepsilon_{\Delta\eta}$ considering as disturbance is suppressed by the sliding mode item $\alpha(t; \hat{x}, y)$. The estimation error $\tilde{\theta}_{\Delta\eta}$ of the unknown parameters tend to zero asymptotically when $t \to \infty$, meaning that the estimation of the volumetric efficiency error $\Delta\eta_v\left(\upsilon|\hat{\theta}_{\Delta\eta}\right)$ obtained by the proposed method satisfying inequality $\left|\Delta\eta_v(\upsilon) - \Delta\eta_v\left(\upsilon|\hat{\theta}_{\Delta\eta}\right)\right| \leq \varepsilon_{\Delta\eta}$ for the any given positive constant $\varepsilon_{\Delta\eta}$. Then, the estimation of the volumetric efficiency error $\Delta\eta_v(\upsilon)$ is achieved by the proposed method, as well as the estimation of the cylinder mass flow $\hat{W}_{ei} = \left(\eta_{vk} + \Delta\eta_v\left(\upsilon|\hat{\theta}_{\Delta\eta}\right)\right) p_{im} n_e V_d \big/ 120 R_a T_{im}$.

TABLE 1. Engine specifications.

Fuel system	Direct injection
Displacement (L)	2
Intake manifold volume (L)	4
Exhaust manifold volume (L)	1.5
Max engine speed (rpm)	7496.418
Calorific value of the gasoline(J/kg)	4.2×10^7
Max power (kW)	176 @ 6515 rpm
Max torque ($N \cdot m$)	287 @ 4095 rpm

III. SIMULATION

In this section, the simulation study of the proposed method to estimate the volumetric efficiency error is presented in the environment of 2.0L R4-cylinder SI gasoline engine from enDYNA provided by Tesis [31], [32], which is a professional software tool for the real-time simulation of internal combustion engines. The specifications of the R4-cylinder SI-engine are given in TABLE 1. In enDYNA, the volumetric efficiency is depending on air density, intake manifold pressure and intake manifold temperature, in which the ambient temperature changes the intake manifold temperature.

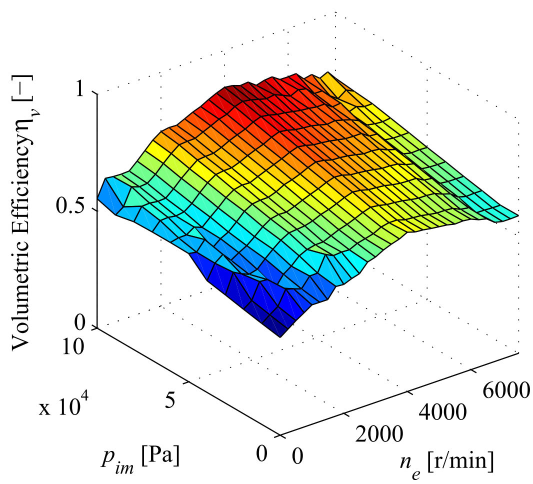

FIGURE 2. The volumetric efficiency map identified from enDYNA data at ambient temperature 20°C.

A. VOLUMETRIC EFFICIENCY ERRORS AT DIFFERENT AMBIENT TEMPERATURES

To analyze the effect of volumetric efficiency error on the model accuracy of the cylinder mass flow at different ambient temperatures, the volumetric efficiency map shown in Fig. 2 is employed as the known model item η_{vk} from Eqs. (3) in this simulation, which is identified at ambient temperature 20°C. Meanwhile, the cold start transient phase of the federal test procedure 75 (FTP75) [33] is used here, under which the throttle angle u_{th}, engine speed n_e, intake manifold pressure p_{im} and vehicle velocity are plotted in Fig. 3.

The comparison between the volumetric efficiency map shown in Fig. 2 and the volumetric efficiency from enDYNA at different ambient temperatures (20°C and −20°C, which are the highest and lowest temperature in enDYNA respectively) is presented in Fig. 4(a). Correspondingly, the comparison between the cylinder mass flow $\hat{W}_{ei}$ computed by volumetric efficiency map and the cylinder mass flow from enDYNA at different ambient temperatures is presented in Fig. 4(b). The mean absolute error between the volumetric efficiency map shown in Fig. 2 and the enDYNA volumetric efficiency is given in TABLE 2, as well as the mean absolute error between the cylinder mass flow $\hat{W}_{ei}$ with the volumetric efficiency map and the enDYNA cylinder mass flow. It demonstrates that the model accuracy of the cylinder mass flow with the volumetric efficiency map identified at ambient temperature 20°C is deteriorated by the volumetric efficiency error $\Delta\eta_v$ at ambient temperature −20°C, which must be compensated to improve the estimation precision of the cylinder mass flow $\hat{W}_{ei}$.

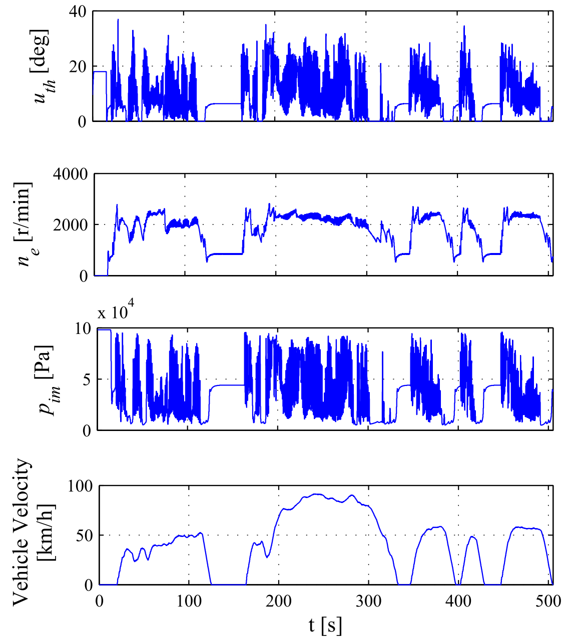

FIGURE 3. Evolution of throttle angle u_{th}, engine speed n_e, intake manifold pressure p_{im} and vehicle velocity under FTP75 cycle.

TABLE 2. Mean absolute error of η_v and W_{ei} at ambient temperatures 20°C and −20°C under FTP75 cycle.

T_{amb} (K)	20°C	-20°C
η_v (-)	0.005	0.0117
W_{ei} (kg/s)	0.00004	0.0002

B. CYLINDER AIR FLOW ESTIMATION

To validate the effectiveness of the proposed method, the observer architecture is illustrated in Fig. 5. Meanwhile, one fuzzy system in the form of (8) is used to approximate the unknown volumetric efficiency error $\Delta\eta_v(\upsilon)$ with $\upsilon = (p_{im}, n_e, T_{amb})$ as input.

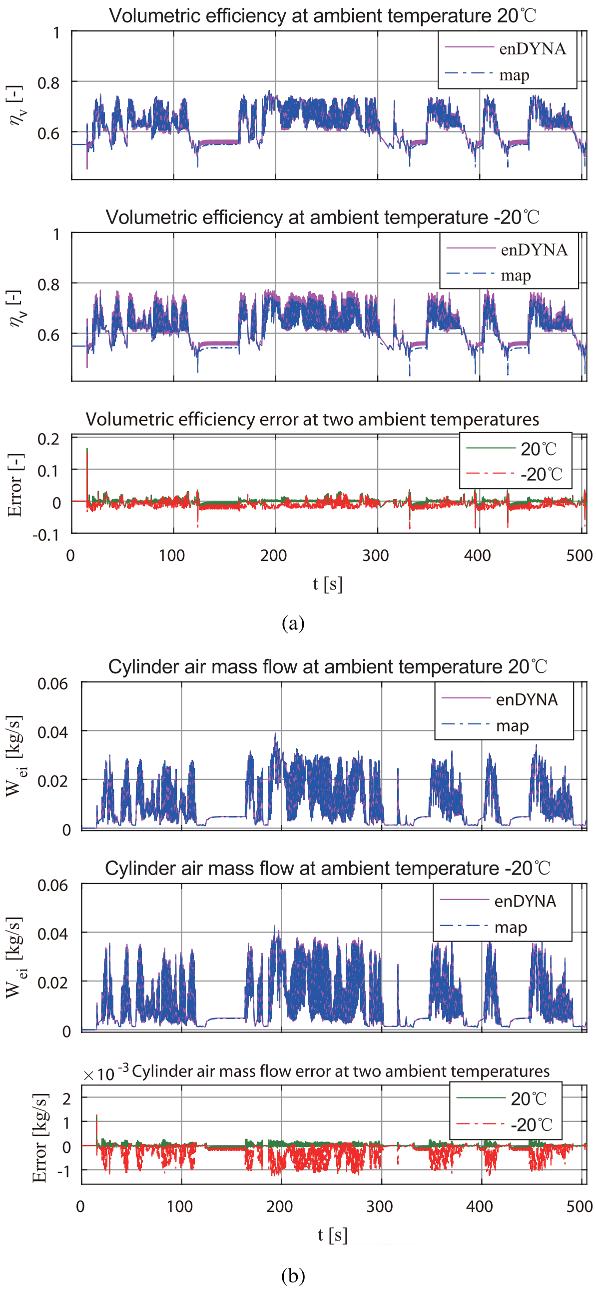

FIGURE 4. Evolution of the volumetric efficiency and cylinder mass flow at ambient temperatures 20°C and −20°C under FTP75 cycle respectively. (a) enDYNA volumetric efficiency, map and errors. (b) enDYNA cylinder mass flow, model using map and errors.

Generally, the fuzzy variables are set in an interval [a, b]. The fuzzy membership functions should be chosen so that they can cover the interval [a, b] of the fuzzy variables uniformly. According to the interval of the fuzzy variables and the chosen number of the fuzzy membership functions, the center can be determined. The width is chosen as a constant by the designer.

According to the range $p_{im} \in [0, 100000]$ and $n_e \in [500, 3000]$ from Fig. 3, the fuzzy membership functions are

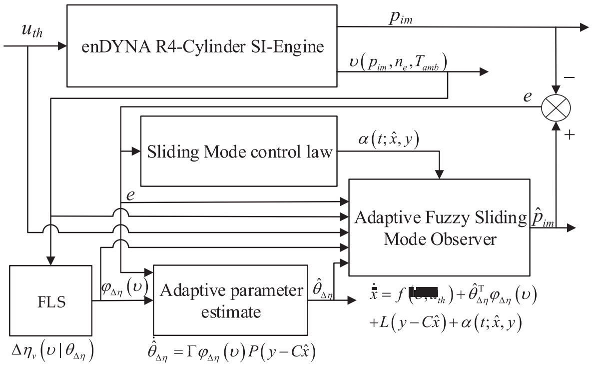

FIGURE 5. Schematic diagram for the estimation of volumetric efficiency error.

defined for each variable υ_i $(i = 1, 2, 3)$ as follows:

$$\mu_{F_1^{k_1}}(\upsilon_1) = \exp\left(-\frac{1}{2}\left(\frac{\upsilon_1 - p_{im,k_1}}{1666}\right)^2\right)$$

$$\mu_{F_2^{k_2}}(\upsilon_2) = \exp\left(-\frac{1}{2}\left(\frac{\upsilon_2 - n_{e,k_2}}{83}\right)^2\right)$$

$$\mu_{F_3^{k_3}}(\upsilon_3) = \exp\left(-\frac{1}{2}\left(\frac{\upsilon_3 - T_{amb,k_3}}{3}\right)^2\right)$$

where

$$p_{im,k_1} \in \{10000k_1 | k_1 = 1, 2, \ldots, 10\}$$
$$n_{e,k_2} \in \{500k_2 | k_2 = 1, 2, \ldots, 6\}$$
$$T_{amb,k_3} \in \{10(k_3 - 4) | k_3 = 1, 2, \ldots, 8\}$$

The lth fuzzy rule is constructed as

R^l: if υ_1 is $F_1^{k_1}$ and $\cdots$ and υ_n is $F_3^{k_3}$, then $\Delta\eta_v$ is G^l where $F_i^{k_i}$ and G^l are fuzzy sets, $i = 1, 2, 3$, $l = 1, 2, \ldots, m$, and $m = 10 \times 6 \times 8 = 480$ is the total number of rules whose IF parts comprise all the possible combinations of the $F_i^{k_i}$'s for $i = 1, 2, 3$.

Denoting $j = 3^2(k_1 - 1) + 3(k_2 - 1) + k_3$, then for k_i, $i = 1, 2, 3$, $j \in \{1, 2, \ldots, 480\}$. Collect j in the ordering for $j = 1, 2, \ldots, 480$, and let

$$\varphi_{\Delta\eta,j}(\upsilon) = \frac{\mu_{F_1^{k_1}}(\upsilon_1)\,\mu_{F_2^{k_2}}(\upsilon_2)\,\mu_{F_3^{k_3}}(\upsilon_3)}{\sum_{l=1}^{480}\mu_{F_1^{k_1}}(\upsilon_1)\,\mu_{F_2^{k_2}}(\upsilon_2)\,\mu_{F_3^{k_3}}(\upsilon_3)}$$

Then, $\varphi_{\Delta\eta}(x) = \left[\varphi_{\Delta\eta,1}(x), \varphi_{\Delta\eta,2}(x), \ldots, \varphi_{\Delta\eta,N}(x)\right]^{\mathrm{T}}$, and we have $\Delta\eta_v\left(\upsilon|\hat{\theta}_{\Delta\eta}\right) = \hat{\theta}_{\Delta\eta}^{\mathrm{T}}\varphi_{\Delta\eta}(\upsilon)$.

The initial values of observer (12) used in the simulation are $\hat{x}(t_0) = 9.8 \times 10^5$ and $\hat{\theta}(t_0) = 0$. The design parameters are chosen as $L = 128$, $\Gamma = 10^{-7} \cdot I$, $P = 0.01$, $l_\alpha = 0.1$, $\varepsilon_\alpha = 10^{-15}$.

Transient condition is different from steady-state operation (i.e., operation at the same engine speed and injected fuel of the respective transient cycles). That is, both the engine speed and the injected fuel change continuously during transient operation [34]. In order to verify the effectiveness of the

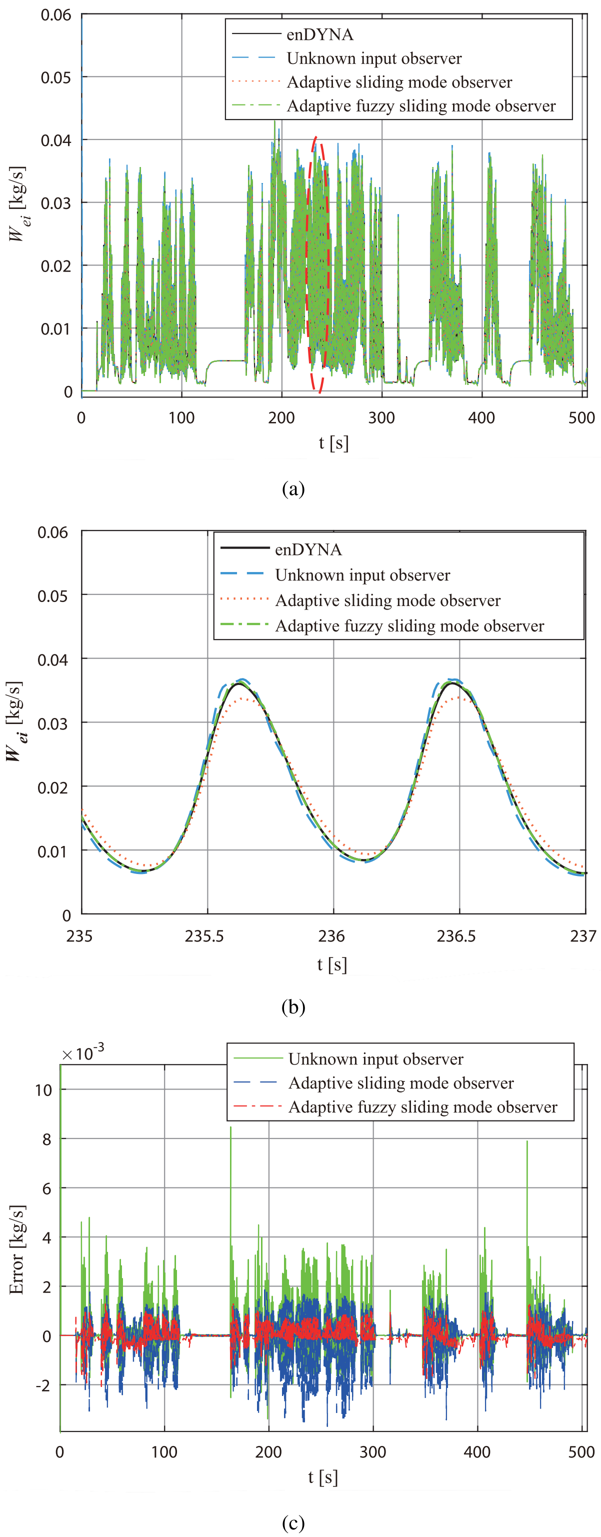

FIGURE 6. Evolution of the estimation of the cylinder mass flow $\hat{W}_{ei}$ at ambient temperature −20°C under FTP75 cycle. (a) Cylinder mass flow estimation; (b) Cylinder mass flow estimation between 235s and 240s; (c) Estimation errors.

presented algorithm, the cold start transient phase of the FTP75 and the urban driving cycle ECE are respectively used as transient conditions in the following.

TABLE 3. Estimation errors of the unknown input observer, sliding mode observer and the proposed method under FTP75 cycle.

	Max abs. error	Mean abs. error
Unknown input observer	0.0085	0.00036
Adaptive sliding mode observer	0.0036	0.00045
Proposed method	0.0018	0.00019

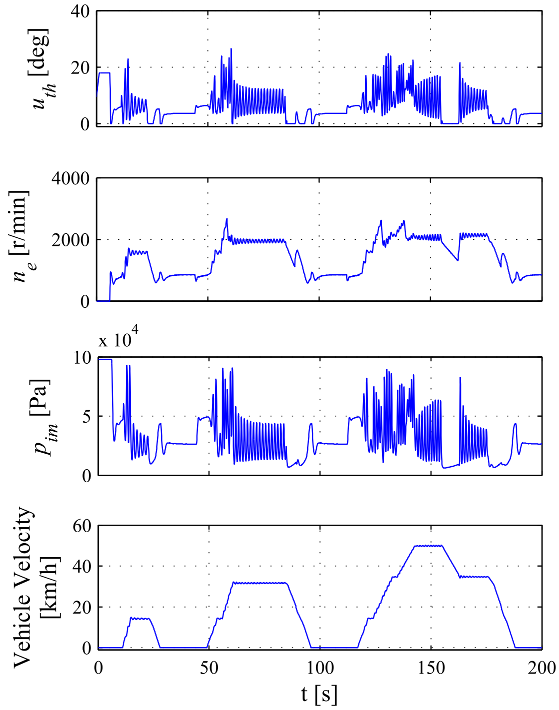

FIGURE 7. Evolution of throttle angle u_{th}, engine speed n_e, intake manifold pressure p_{im} and vehicle velocity under ECE cycle.

Under the cold start transient phase of the FTP75 at ambient temperature −20°C, the comparison of the cylinder mass flow $\hat{W}_{ei}$ from the unknown input observer [17], adaptive sliding mode observer [22], and proposed adaptive fuzzy sliding mode observer is presented in Fig. 6, in which the volumetric efficiency shown in Fig. 2 is used as the modeled term η_{vk}. Accordingly, the maximum absolute error and mean absolute error of these three estimation approaches against the enDYNA signal are given in TABLE 3. It is demonstrating that the estimation precision of the cylinder mass flow $\hat{W}_{ei}$ using the proposed approach is improved noticeably under FTP75.

To verify the effectiveness of the presented algorithm under other driving cycle condition, one segment of urban driving cycle ECE (Economic Commission for Europe) is used here [35], under which the throttle angle u_{th}, engine speed n_e, intake manifold pressure p_{im} and vehicle velocity are plotted in Fig. 7. Accordingly, the comparison of the cylinder mass flow from the unknown input observer, adaptive sliding mode observer and proposed adaptive fuzzy sliding mode observer is presented in Fig. 8, in which the volumetric efficiency shown in Fig. 2 is also used as the modeled term η_{vk}.

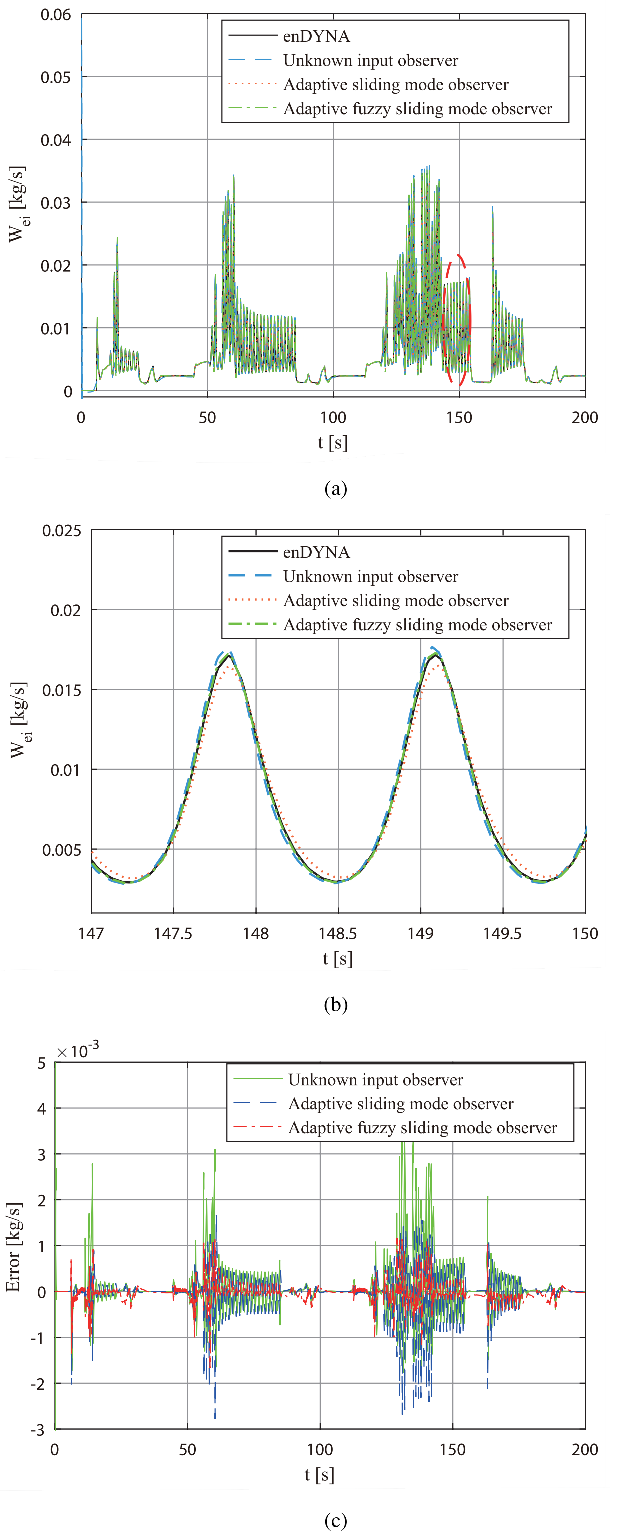

FIGURE 8. Evolution of the estimation of the cylinder mass flow $\hat{W}_{ei}$ at ambient temperature −20°C under ECE cycle. (a) Cylinder mass flow estimation; (b) Cylinder mass flow estimation between 147s and 150s; (c) Estimation errors.

Accordingly, the maximum absolute error and mean absolute error of these three estimation approaches against the enDYNA signal are given in TABLE 4. It is demonstrating that the estimation precision of the cylinder mass flow using the proposed approach is improved obviously under ECE cycle.

TABLE 4. Estimation errors of the unknown input observer, sliding mode observer and the proposed method under ECE cycle.

	Max abs. error	Mean abs. error
Unknown input observer	0.0033	0.00020
Adaptive sliding mode observer	0.0025	0.00022
Proposed method	0.0014	0.00011

IV. CONCLUSION

An efficient method to improve the estimation precision of the engine cylinder mass flow under transient condition was developed in a 4-stroke SI gasoline engine. A FLS with unknown parameters was employed to approximate the volumetric efficiency error. With the combination of the FLS regression model and SI gasoline engine air path dynamic model, an adaptive fuzzy sliding mode observer was designed to jointly estimate state and unknown parameters, as well as suppress the disturbance from the FLS approximation error, thus improving the estimation precision of the cylinder mass flow, compared with the method of both the unknown input observer [17] and adaptive sliding mode observer [22]. Under the cold start transient phase of the FTP75 and the urban driving cycle ECE, the effectiveness of the proposed method was validated and verified in the engine software enDYNA. The results demonstrate that the estimation precision of the cylinder mass flow can be obviously improved by the presented method under transient conditions.

REFERENCES

[1] Y. Zhao *et al.*, "Reducing secondary organic aerosol formation from gasoline vehicle exhaust," *Proc. Nat. Acad. Sci. USA*, vol. 114, no. 27, pp. 6984–6989, 2017.

[2] G. Saliba *et al.*, "Comparison of gasoline direct-injection (GDI) and port fuel injection (PFI) vehicle emissions: Emission certification standards, cold-start, secondary organic aerosol formation potential, and potential climate impacts," *Environ. Sci. Technol.*, vol. 51, no. 11, pp. 6542–6552, 2017.

[3] C. Wang and Z. Liu, "Adaptive sliding mode observer for updating maps with an application to mass air flow sensors in diesel engines," *Trans. Inst. Meas. Control*, vol. 39, no. 12, pp. 1885–1897, 2017.

[4] J. B. Heywood, *Internal Combustion Engine Fundamentals*, vol. 930. New York, NY, USA: McGraw-Hill, 1988.

[5] C. Onder and L. Guzzella, *Introduction to Modeling and Control of Internal Combustion Engine Systems*. Berlin, Germany: Springer-Verlag, 2004.

[6] J. Lauber, T. M. Guerra, and M. Dambrine, "Air-fuel ratio control in a gasoline engine," *Int. J. Syst. Sci.*, vol. 42, no. 2, pp. 277–286, 2011.

[7] B. A. Al-Himyari, A. Yasin, and H. Gitano, "Review of air-fuel ratio prediction and control methods," *Asian J. Appl. Sci.*, vol. 2, no. 4, pp. 471–478, 2014.

[8] Z. Wang, Q. Zhu, and R. Prucka, "A review of spark-ignition engine air charge estimation methods," SAE Tech. Paper 2016-01-0620, 2016.

[9] B. He, T. Shen, J. Kako, and M. Ouyang, "Input observer-based individual cylinder air-fuel ratio control: Modelling, design and validation," *IEEE Trans. Control Syst. Technol.*, vol. 16, no. 5, pp. 1057–1065, Sep. 2008.

[10] W. W. Pulkrabek, *Engineering Fundamentals of the Internal Combustion Engine*. Upper Saddle River, NJ, USA: Prentice-Hall, 2004.

[11] E. Hendricks and S. C. Sorenson, "Mean value modelling of spark ignition engines," SAE Tech. Paper 900616, 1990.

[12] C. Wang, J. Gao, and M. Liang, "Identification of look-up tables using gradient algorithm," *ISA Trans.*, vol. 75, pp. 64–75, Apr. 2018.

[13] G. De Nicolao, R. Scattolini, and C. Siviero, "Modelling the volumetric efficiency of ic engines: Parametric, non-parametric and neural techniques," *Control Eng. Pract.*, vol. 4, no. 10, pp. 1405–1415, 1996.

[14] G. W. Malaczynski, M. Müller, J. Pfeiffer, D. Cabush, and K. Hoyer, "Replacing volumetric efficiency calibration look-up tables with artificial neural network-based algorithm for variable valve actuation," SAE Tech. Paper 2010-01-0158, 2010.

[15] N. Müller, M. Hafner, and R. Isermann, "A neuro-fuzzy based method for the design of combustion engine dynamometer experiments," SAE Tech. Paper 2000-01-1262, 2000.

[16] M. Neve, G. D. Nicolao, G. Prodi, and C. Siviero, "Estimation of engine maps: A regularized basis-function networks approach," *IEEE Trans. Control Syst. Technol.*, vol. 17, no. 3, pp. 716–722, May 2009.

[17] A. Stotsky and I. Kolmanovsky, "Application of input estimation techniques to charge estimation and control in automotive engines," *Control Eng. Pract.*, vol. 10, no. 12, pp. 1371–1383, Dec. 2002.

[18] A. Stotsky, I. Kolmanovsky, and S. Eriksson, "Composite adaptive and input observer-based approaches to the cylinder flow estimation in spark ignition automotive engines," *Int. J. Adapt. Control Signal Process.*, vol. 18, no. 2, pp. 125–144, 2004.

[19] J. Fei and H. Ding, "Adaptive sliding mode control of dynamic system using RBF neural network," *Nonlinear Dyn.*, vol. 70, no. 2, pp. 1563–1573, Oct. 2012.

[20] J. Fei and C. Lu, "Adaptive fractional order sliding mode controller with neural estimator," *J. Franklin Inst.*, vol. 355, pp. 2369–2391, Mar. 2018.

[21] C. Fei and J. Lu, "Adaptive sliding mode control of dynamic systems using double loop recurrent neural network structure," *IEEE Trans. Neural Netw. Learn. Syst.*, vol. 29, no. 4, pp. 1275–1286, Apr. 2018.

[22] V. H. Monir, R. Salehi, H. Salarieh, A. Alasty, and G. Vossoughi, "Real-time estimation of the volumetric efficiency in spark ignition engines using an adaptive sliding-mode observer," *Proc. Inst. Mech. Eng. D, J. Automobile Eng.*, vol. 229, no. 14, pp. 1925–1933, 2015.

[23] M. Davanipoor, M. Zekri, and F. Sheikholeslam, "Fuzzy wavelet neural network with an accelerated hybrid learning algorithm," *IEEE Trans. Fuzzy Syst.*, vol. 20, no. 3, pp. 463–470, Jun. 2012.

[24] H. H. YusefSa'ad, N. A. M. Isa, M. M. Ahmed, and A. H. YusefSa'd, "A robust structure identification method for evolving fuzzy system," *Expert Syst. Appl.*, vol. 93, pp. 267–282, Mar. 2017.

[25] G. Lai, Z. Liu, Y. Zhang, C. L. P. Chen, S. Xie, and Y. Liu, "Fuzzy adaptive inverse compensation method to tracking control of uncertain nonlinear systems with generalized actuator dead zone," *IEEE Trans. Fuzzy Syst.*, vol. 25, no. 1, pp. 191–204, Feb. 2017.

[26] S. Tong and Y. Li, "Adaptive fuzzy output feedback tracking backstepping control of strict-feedback nonlinear systems with unknown dead zones," *IEEE Trans. Neural Netw.*, vol. 20, no. 1, pp. 168–180, Feb. 2012.

[27] L.-X. Wang, "Stable adaptive fuzzy control of nonlinear systems," *IEEE Trans. Fuzzy Syst.*, vol. 1, no. 2, pp. 146–155, May 1993.

[28] H. Zhang, G. Zhang, and J. Wang, "$\mathcal{H}_\infty$ observer design for LPV systems with uncertain measurements on scheduling variables: Application to an electric ground vehicle," *IEEE/ASME Trans. Mechatronics*, vol. 21, no. 3, pp. 1659–1670, Jun. 2016.

[29] H. Zhang and J. Wang, "Adaptive sliding-mode observer design for a selective catalytic reduction system of ground-vehicle diesel engines," *IEEE/ASME Trans. Mechatronics*, vol. 21, no. 4, pp. 2027–2038, Aug. 2016.

[30] J. J. E. Slotine and W. Li, *Applied Nonlinear Control*. China Machine Press, 2004.

[31] T. Dynaware, "en-DYNA THERMOS 2.0 block reference manual," Tech. Rep., Jun. 2006.

[32] T. Dynaware, "en-DYNA THERMOS 2.0 block user manual," Tech. Rep., 2006.

[33] *Protection of the Environment. Code of Federal Regulations, Part 86*.

[34] C. D. Rakopoulos and E. G. Giakoumis, *Diesel Engine Transient Operation: Principles of Operation and Simulation Analysis*. London, U.K.: Springer-Verlag, 2009.

[35] *Emission Test Cycles for the Certification of Light Duty Vehicles in Europe*, document EEC Directive 90/C81/01, 2009.

CHANGHUI WANG received the Ph.D. degree in control science and engineering from the Harbin Institute of Technology, Harbin, China, in 2016.

He has been with the School of Electromechanical and Automotive Engineering, Yantai University, Yantai, China, since 2017. His current research interests include automotive engine, system identification, adaptive control, and intelligent systems and control.

MEI LIANG received the Ph.D. degree in control science and engineering from the Harbin Institute of Technology, Harbin, China, in 2017.

He has been with the School of Electromechanical and Automotive Engineering, Yantai University, Yantai, China, since 2017. His current research interests include automotive engine, system identification, adaptive control, and intelligent systems and control.

CHUN-NA LI received the master's and Ph.D. degrees from the Department of Mathematics, Harbin Institute of Technology, China, in 2009 and 2012, respectively.

She is currently an Associate Professor with the Zhijiang College, Zhejiang University of Technology. Her research interests include data mining, machine learning, and optimization methods.